JOURNAL OF MATERIALS SCIENCE **38** (2003) 3051–3054

Effects of methane partial pressure on synthesis of single-walled carbon nanotubes by chemical vapor deposition

WEIFENG LIU, WEILI CAI*, LIANZENG YAO, XIAOGUANG LI
Department of Materials Science and Engineering, University of Science and Technology of China, Hefei, Anhui 230026, People's Republic of China
E-mail: wlcai@ustc.edu.cn

ZHEN YAO
Department of Physics, University of Texas at Austin, TX 78712-1081, USA

A series of experiments have been done to investigate the role of methane partial pressure in the synthesis of carbon nanotubes by catalyst chemical vapor deposition. It is supposed that there is a critical methane partial pressure (~0.4 atm) for single-walled carbon nanotube (SWNT) synthesis at 850°C. When the methane partial pressure is higher than the critical value, the whole rate is decided by the carbon diffusion rate on the catalyst surface or in the bulk, contrariwise, the synthesis rate is proportional to the methane partial pressure.

1. Introduction

Carbon nanotubes [1–3] are novel materials with extraordinary mechanical [4, 5] and unique electronic [6–8] properties. They have attracted much attention in recent years for their potential applications in nanoelectronics [9], field emission devices [6, 10], scanning probes and sensors [11–13], high strength composites etc. [14]. These materials have been synthesized by a variety of techniques including electric arc-discharge [15], laser ablation [16] and chemical vapor deposition (CVD) [17–19]. Both the arc- and the laser-based methods involve evaporation of carbon at ~3000°C, which makes it difficult to control the growth conditions, and therefore these processes typically operate in a batch mode and are poorly suited to large volume and low cost production. In contrast, the CVD method presently represents the best hope for large scale production of nanotube materials. By utilizing carbon-rich gases as carbon feedstock, CVD of various hydrocarbon gases on transition-metal catalysts has been successful in obtaining carbon fibers and carbon nanotubes, and it is easy to control the synthesis conditions. However, there are usually rich-defect nanotubes and other byproducts such as fullerenes and amorphous carbon in the CVD products, so it is still a challenge work to prepare high quality nanotubes in large scale.

Much attention has been focused on the influence of the catalyst, substrate [17] and reaction temperature [18], which are critical for the synthesis of carbon nanotubes by CVD. Only a few works on the influence of the source gas have been reported in the literature. Choi *et al.* [20] have studied the effects of ammonia on the alignment of carbon nanotubes in an ambient pressure thermal chemical vapor deposition assisted by Ni. They have suggested that ammonia plays a role of inhibiting the formation of amorphous carbons during reaction. In this paper, the effect of the methane partial pressure (MPP) on the formation and quality of SWNTs is reported.

2. Experimental

Catalysts used in our experiments were prepared using a sol-gel technique. In a typical experiment [18], 23 g ASB was dissolved in 200×10^{-6} m^3 ethanol in a round bottom flash under a reflux condition. Then, 10^{-7}m^3 concentrated HNO_3 diluted with 10^{-6} m^3 water and 50×10^{-6} m^3 ethanol was added into the mixture. It was refluxed for 1 h, and then 1.7 g $Fe_2(SO_4)_3 \cdot XH_2O$ was added into the mixture (molar ratio Fe:Al = 1:16). After refluxing for another two hours, the mixture was cooled to room temperature, and 5×10^{-6} m^3 concentrated NH_4OH diluted with 5×10^{-6} m^3 of water was added into the mixture. A gel was formed and aged at room temperature for 10 h. After that, it was dried at 60°C for 24 h, and then ground to powder.

For methane CVD experiment, a vessel containing about 10 mg of the catalyst-embedded powder was placed in a quartz tube mounted in a tube furnace. The quartz tube was vacuumized to1.3 Pa, and then argon gas passed through the quartz tube. As the temperature was raised to 850°C, the reaction gas (methane or methane/carrier gas) replaced the argon gas. The flow rate of methane was kept at 200 sccm. The reaction

* Author to whom all correspondence should be addressed.

lasted for 30 min, then the furnace was switched off and the argon replaced the reaction gas again during furnace cooling.

The morphology of carbon nanotubes was investigated using a transmission electron microscope (TEM, Hitachi H800) and a high-resolution transmission electron microscope (HRTEM, JEOL-2010). Samples for TEM observations were prepared by sonicating ~2 mg synthesized materials in 10^{-5} m^3 methanol for half an hour. A few drops of the resulting suspension were put onto a holy-carbon TEM grid. The acceleration voltage of the electron beam was 200 kV. Raman spectrum measurements were performed on a Raman spectrometer (SPEX Ramalog 6) using 10 mW of 514 nm line of an Ar ion laser.

3. Results and discussion

The growth process of carbon nanotubes by CVD with catalyst usually includes three steps: (1) dissociation of hydrocarbon gas on the surface of catalyst and then producing hydrogen and carbon atoms; (2) the carbon atoms diffuse either on the surface or through the bulk of the catalyst; (3) the growth of these carbon atoms into nanotubes. The hydrocarbon gas decomposes at high temperatures without the assistance of catalyst at the same time, which produces a lot of undesired amorphous carbons. Consequently, what we should do is to restrain the high-temperature dissociation of hydrocarbon gas and to reduce the content of amorphous carbons in the products.

Fig. 1 shows the TEM image of product synthesized at 850°C using CH_4 or CH_4/Ar as the reacting gas with methane flux of 200 sccm. The flocs shown in the picture are the catalyst and alumina gels. Comparing Fig. 1a to b and c, it can be seen that the carbon nanotubes in Fig. 1b and c are cleaner than in Fig. 1a. In contrast, without the carrier gas, Ar, large amount of amorphous carbons have been produced and attached on the nanotubes, which compose a triangle, as displayed in Fig. 1a. Some of the amorphous carbons disappeared during TEM observation as the irradiation time lasted longer. A similar phenomenon has also been observed when hydrogen instead of argon is used as the carrier gas (not shown here). It indicates that the inhibiting effect on the methane decomposition at high temperatures has nothing to do with the carrier gas, which should be attributed to the decrease of methane partial pressure.

The walls of SWNTs in Fig. 1b and c are very straight and clean, free of any amorphous carbons attached on them, which is in accordance with the TEM observation results presented in Fig. 1a. Fig. 1b exhibits some individual SWNTs with different diameters, the largest one of which is about 5 nm. Fig. 1c demonstrates a megascopic SWNT bundle. It can be seen that the diameter distribution of the SWNTs is rather narrow, which focuses on about 0.80 nm.

Raman spectroscopy is a powerful technique for characterizing the structure of carbon nanotubes [21]. There are two phonon modes that give strong Raman patterning: the radial breathing mode (RBM) near 190 cm^{-1} and the tangential C–C mode (G band), which is related to the Raman-allowed phonon mode E_{2g} and involves out-of-phase intralayer displacement in the grapheme structure of the nanotube, at about 1580 cm^{-1}. The RBM frequency is predicted to depend

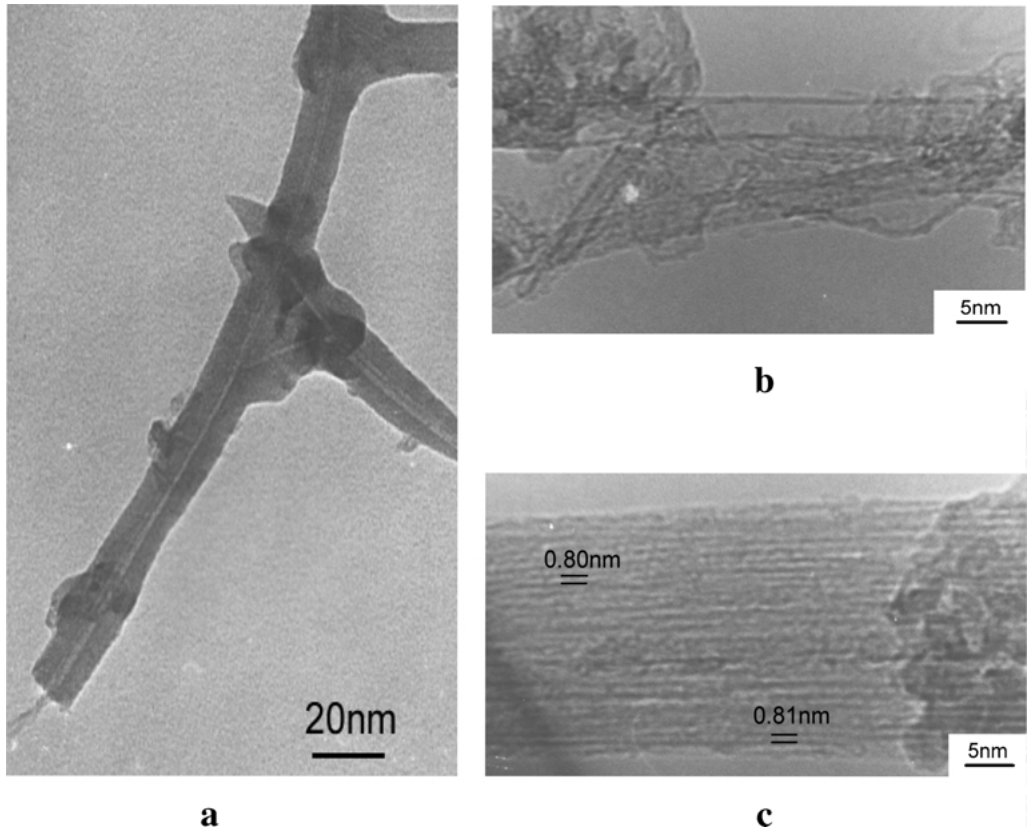

Figure 1 Transmission electron microscope images of carbon nanotubes formed at 850°C using different methane partial pressure: (a) CH_4, (b) CH_4/Ar, and (c) CH_4/Ar.

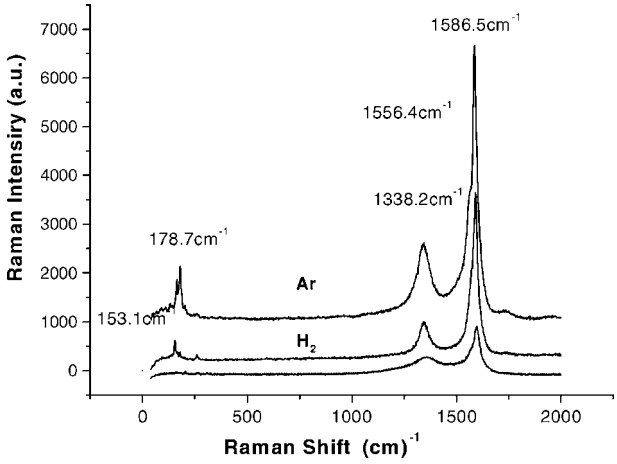

Figure 2 Raman spectra from samples grown by CVD with different carrier gas. The labels show the carrier gas, and the methane is kept at 200 sccm.

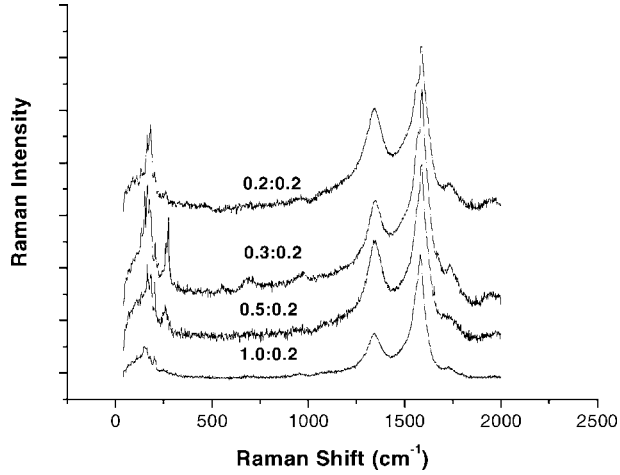

Figure 3 Raman spectra from samples grown by CVD with different methane partial pressure. The methane flux is kept at 200 sccm.

sensitively on the diameter of the tubes [22]. It provides information about the electronic properties of the tubes and is a measure of the presence of ordered carbon. The so-called D band at around 1350 cm^{-1} is related to amorphous carbon and defects of the nanotube. The size of the D band relative to the G band can be used as a qualitative measurement for the formation of undesired forms of carbon. The radial A_{1g} breathing mode frequency range (RMB) can offer the information of the distribution of the single-walled or double-walled nanotubes.

Fig. 2 shows the Raman spectra for samples using different carrier gas with a methane flowrate of 200 sccm. For material synthesized without a carrier gas, the Raman spectrum shows a broad, weak feature at 1338 cm^{-1} (the 'D' band), and a well-known feature at 1596.5 cm^{-1} (the 'G' band). No peak appears near 190 cm^{-1}. The result indicates that only poorly organized caobon nanotubes with a lot of byproducts are formed as MPP = 1.0 atm.

As a hydrogen flow rate of 300 sccm is introduced, the Raman spectrum reveals a well-known sharp feature at 1586.5 cm^{-1} with a shoulder at 1556.4 cm^{-1}, which is expected for resonantly enhanced SWNTs, and a feature at 153 cm^{-1} corresponding to radial breathing vibration modes (RBM). When the hydrogen is replaced by argon, the Raman spectrum shows even stronger peaks at the same features. The intensity of the G band increases rapidly, which indicates the yield and the quality of SWNTs have greatly improved. From the Raman spectra for samples using hydrogen or argon as the carrier gas, it can be seen that both the ratios of the G band intensity to the D band are near 5:1. It indicates that the hydrogen has the same inhibiting effect on SWNTs and amorphous carbons as the argon does.

Fig. 3 displays Raman spectra for samples with different MPP. Apparently, with decrease of the MPP, the graphitization degree of samples increases first, and then drops. Therefore, the optimum MMP of about 0.4 atm in our experiments can be obtained, under which the intensities of the G band (at 1586 cm^{-1}) and the RBM (at 153 cm^{-1}) are strongest.

It is known, there are two chemical reactions in methane chemical vapor deposition: the high-temperature decomposition and the catalyst-assistant one:

$$CH_4(g) \xrightarrow{\text{high-temperature}} C(s)^* + 2H_2(g)$$

$$CH_4(g) \xrightarrow{\text{high-temperature,catalyst}} C(s)^{**} + 2H_2(g)$$

where C* represent amorphous carbons, and C** denote the carbon atoms which are adsorbed on the catalyst. When the carbon atoms in the catalyst are saturated, nanotubes will grow from the bulk. Hence, apart from the decomposition rate of the methane in the catalyst, the diffusion rate of carbon atoms is also essential to synthesis of carbon nanotubes. As a result, there should be a critical methane partial pressure under which the diffusion rate of carbon atoms is equal to the catalyst-assisted decomposition rate. When the methane partial pressure is higher than the critical value, it is supposed that the catalyst-assisted decomposition rate of the methane is a constant independent of the MPP at a certain temperature. The diffusion rate of carbon atoms in the catalyst bulk is also nearly a constant in our experiment at the same time. At the same time, the high-temperature decomposition rate is proportional to the methane partial pressure. When the MPP rises, the high-temperature decomposition rate increases, but the catalyst-assisted decomposition rate and the diffusion rate keep unchanged. It will produce extra carbon atoms and undesired amorphous carbons will be formed. When the methane partial pressure is below the critical value, the synthesis is determined by the catalyst-assisted decomposition rate, which is proportional to the methane partial pressure. As the MPP decreases, the catalyst-assisted decomposition drops more rapidly than the high-temperature decomposition, and the difference between the high-temperature decomposition rate and the catalyst-assisted one gets closer (see Fig. 4). From our experiment data, it is supposed that the critical methane partial pressure at 850°C is 0.4 atm under which the difference between the catalyst-assisted decomposition rate and the high-temperature one is

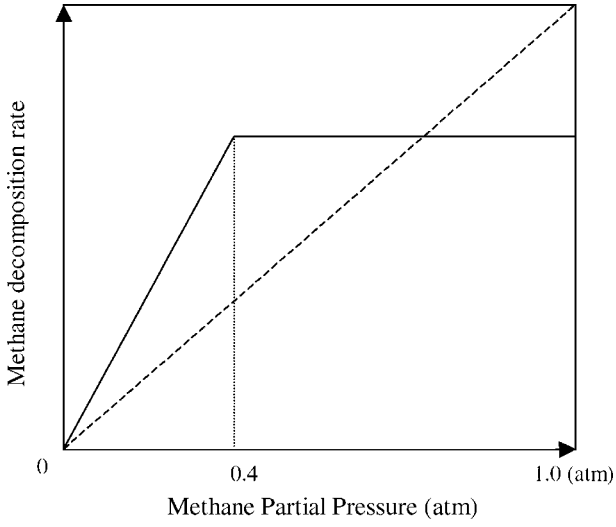

Figure 4 Schematic diagram of MPP dependence of high-temperaturea and catalyst-assistant decomposition rate: (————), Catalyst-assistant Decomposition; (---------), High-temperature Decomposition.

the largest, and the inhibiting effect is the most effective.

According to the theoretical calculations, the RBM frequency depends only on the diameter of a SWNT, d, and can be predicted by the following expression [23]:

$$\upsilon\,(\mathrm{cm}^{-1}) = 223.75\,(\mathrm{cm}^{-1}\cdot\mathrm{nm})/\mathrm{d}\,(\mathrm{nm}).$$

Therefore, the size distribution of SWNTs can be estimated from RBM frequencies in the Raman spectrum by the expression. In Fig. 4, two peaks at 165 and 276 cm^{-1} are identified as the RBM of SWNTs with diameters of 1.36 and 0.81 nm, respectively. By comparison with the HRTEM images, it is obvious that SWNTs with diameter of 0.81 nm lie in bundles and those with 1.36 nm as individuals. It can be seen that the bundle SWNTs have a very narrow size distribution, and the diameter obtained from the HRTEM image and the Raman spectrum is in accordance with each other. On the contrary, the individual SWNTs observed from the HRTEM image have a wide size distribution due to a small area investigated resulting in a large fluctuation. And, the diameters obtained from the HRTEM image and the Raman spectrum have a large difference. As the MPP decreases, the intensities of the RBM peaks of SWNTs also change a lot, especially the peak at 276 cm^{-1}. But, the reason why the diameters of bundle SWNTs are sensitive to the MPP is still under investigation.

4. Conclusions

The role of the methane partial pressure (MPP) in the synthesis of single-walled carbon nanotubes (SWNTs) using the atmospheric CVD method was investigated. The quality and the quantity of SWNTs have greatly been improved by optimzing the flux of the carrier gas. It is supposed that there is a critical MPP ($\sim$0.4 atm) for SWNT synthesis by CVD at 850°C. When the MPP is higher than the critical value, the synthesis is determined by the carbon diffusion rate on the catalyst surface or in the bulk, contrariwise, the synthesis rate is proportional to the MPP.

Acknowledgments

This work is supported by the National Natural Science Foundation of China (NSFC) under grant No. 50128202.

References

1. S. IIJIMA, *Nature* **354** (1991) 56.
2. S. IIJIMA and T. ICHIHASHI, *ibid.* **363** (1993) 603.
3. A. C. DILLON, K. M. JONES, T. A. BEKKEDAHL, C. H. KIANG, D. S. BETHUNE and M. J. HEBEN, *ibid.* **386** (1997) 377.
4. M. M. J. TREACY, T. W. EBBESEN and J. M. GIBSON, *ibid.* **381** (1996) 678.
5. D. A. WALTERS, L. M. ERICSON, M. J. CASAVANT, J. LIU, D. T. COLBERT, K. A. SMITH and R. E. SMALLEY, *Appl. Phys. Lett.* **74** (1999) 3803.
6. W. A. DE HEER, A. CHATELAIN and D. UGARTE, *Science* **270** (1995) 1179.
7. W. ZHU, C. BOWER, O. ZHOU, G. KOCHANSKL and S. JIN, *Appl. Phys. Lett* **75** (1999) 873.
8. S. FAN, M. G. CHAPLINE, N. M. FRANKLIN, T. W. TOMBLER, A. M. CASSELL and H. J. DAI, *Science* **283** (1999) 512.
9. S. J. TANS, A. R. M. VERSCHUEREN and C. DEKKER, *Nature* **393** (1998) 49.
10. P. G. COLLINS and A. ZETTL, *Appl. Phys. Lett.* **69** (1996) 1969.
11. R. SERVICE, *Science* **281** (1998) 940.
12. H. J. DAI, J. H. HAFNER, A. G. RINZLER, D. T. COLBERT and R. E. SMALLEY, *Nature* **384** (1996) 147.
13. S. S. WONG, J. D. HARPER, P. T. LANSBURY and C. M. LIEBER, *J. Amer. Chem. Soc.* **120** (1998) 603.
14. C. LIU, Y. Y. FAN, M. LIU, H. T. CONG, H. M. CHENG and M. S. DRESSELHAUS, *Science* **286** (1999) 1127.
15. D. S. BETHUNE, C. H. KIANG, M. S. DEVRIES, G. GORMAN, R. SAVOY, J. VAZQUEZ and R. BEYERS, *Nature* **363** (1993) 605.
16. A. THESS, R. LEE, P. NIKOLAEV, H. J. DAI, P. PETIT, J. ROBERT, C. H. XU, Y. H. LEE, S. G. KIM, A. G. RINZLER, D. T. COLBERT, G. E. SCUSERIA, D. TOMANEK, J. E. FISCHER and R. E. SMALLEY, *Science* **273** (1996) 483.
17. K. JING, A. M. CASSELL and H. DAI, *Chem. Phys. Lett.* **292** (1998) 567.
18. M. SU, B. ZHENG and J. LIU, *ibid.* **322** (2000) 321.
19. G. L.HORNYAK, L. GRIGORIAN, A. C. DILLON, P. A. PARILLA, K. M. JONES and M. J. HEBEN, *J. Phys. Chem.* B **106** (2002) 2821.
20. C. S. CHOI, Y. S. CHO, S. Y. HONG, J. B. PARK and D. J. KIM, *J. Eur. Ceram. Soc.* **21** (2001) 2095.
21. A. M. RAO, E. RICHTER, S. BANDOW, B. CHASE, P. C. EKLUND, K. A. WILLIAMS, S. FANG, K. R. SUBBASWAMY, M. MENON, A. THESS, R. E. SMALLEY, G. DRESSELHAUS and M. S. DRESSELHAUS, *Science* **275** (1997) 187.
22. R. SAITO, T. TAKEYA, T. KIMURA, G. DRESSELHAUS and M. S. DRESSELHAUS, *Phys. Rev.* B **57** (1998) 4145.
23. Z. H. YU and E.B. LOUIS, *J. Phys. Chem.* A **104** (2000) 10995.

Received 11 November 2002
and accepted 9 April 2003